IN-34
185534
31 P

NASA Contractor Report 191511

ICASE Report No. 93-51

# ICASE

20 Years of Excellence

## DEVELOPMENT OF A RECURSION RNG-BASED TURBULENCE MODEL

Ye Zhou

George Vahala

S. Thangam

National Aeronautics and
Space Administration

**Langley Research Center**
Hampton, Virginia 23681-0001

# ICASE Fluid Mechanics

Due to increasing research being conducted at ICASE in the field of fluid mechanics, future ICASE reports in this area of research will be printed with a green cover. Applied and numerical mathematics reports will have the familiar blue cover, while computer science reports will have yellow covers. In all other aspects the reports will remain the same; in particular, they will continue to be submitted to the appropriate journals or conferences for formal publication.

# DEVELOPMENT OF A RECURSION *RNG* – BASED TURBULENCE MODEL[†]

Ye Zhou

ICASE, NASA Langley Research Center

Hampton, Virginia 23681

George Vahala

College of William and Mary

Williamsburg, Virginia 23185

S. Thangam

Stevens Institute of Technology

Hoboken, New Jersey 07030

## ABSTRACT

Reynolds stress closure models based on the recursion renormalization group theory are developed for the prediction of turbulent separated flows. The proposed model uses a finite wavenumber truncation scheme to account for the spectral distribution of energy. In particular, the model incorporates effects of both local and nonlocal interactions. The nonlocal interactions are shown to yield a contribution identical to that from the $\epsilon -RNG$, while the local interactions introduce higher order dispersive effects. A formal analysis of the model is presented and its ability to accurately predict separated flows is analyzed from a combined theoretical and computational stand point. Turbulent flow past a backward facing step is chosen as a test case and the results obtained based on detailed computations demonstrate that the proposed recursion $-RNG$ model with finite cut-off wavenumber can yield very good predictions for the backstep problem.

# 1. INTRODUCTION

Turbulent flows of scientific and engineering importance are characterized by a broad spectrum of length and time scales. While the physical aspects of turbulent flows are best described by the equations of motion, limitations in computer capacity and speed preclude their direct solution for complex flows of relevance to technical applications. The current practice for high Reynolds number flows of practical interest therefore involves some type of modeling for Reynolds stresses. The commonly used turbulence models are based on the calculation of one-point first and second moments such as the mean velocity, mean pressure and turbulent kinetic energy. Among these, the two-equation turbulence models that involve the use of transport equations for the turbulent field parameters that involve the length and the time scales are probably the most widely used. They involve the simplest level of Reynolds stress closure that do not depend specifically on the flow geometry. (For an excellent review of recent trends in analytical methods for Reynolds stress closure, the reader is referred to Speziale.[1])

In its standard form the two-equation Reynolds stress turbulence models involve the turbulence kinetic energy and dissipation based on a Boussinesq type approximation[2] of the form

$$\tau_{ij} = -\frac{2}{3}K\delta_{ij} + \nu_T\left(\frac{\partial U_i}{\partial x_j} + \frac{\partial U_j}{\partial x_i}\right)$$

wherein $U$ is the mean velocity based on Reynolds average, $K$ is the turbulence kinetic energy, and $\nu_T$ is the eddy viscosity which is isotropic. Such a representation of turbulence is often not effective from both theoretical as well as phenomenological point of view and the shortcomings associated with it are fully discussed by Speziale.[1] To over come some of these, models that are nonlinear (i.e., quadratic) in the mean strain rate were proposed in the form of a constitutive relation.[3,4] Speziale[3] employed tensor and dimensional analysis, together with invariance constraints, to derive his model. Yoshizawa's model[4] was obtained by appealing to a two-scale direct interaction approximation. The application of these models depend on the empirical evaluation of the model constants. Apart from the specific values of the constants in these models, these two models have quite similar structure and both were able to predict the anisotropy in the Reynolds stresses in a noncircular duct problem.

The present study addresses the need for a more effective approach in the development of two-equation turbulence models, and in this context the renormalization group (RNG) theory based models are examined for further development. While the application of renormalization group theory to turbulence has attracted much attention,[5-18] it is important to realize that these calculations fall into two distinct categories: (a) $\in$-RNG[5-9], pioneered by Forster et. al.[14], and (b) recursion-RNG,[10-13] pioneered by Rose.[15] These techniques have been critiqued[6,16-18] and compared.[12]

Here, we wish to point out that in the $\epsilon$ -*RNG*, a small parameter $\epsilon$ is introduced into the exponent of the forcing correlation function (with the forcing function being introduced into the momentum equation). The theory is then developed for $\epsilon \ll 1$, and all constants generated are evaluated in this limit $\epsilon \ll 1$. However, at the same time, all exponents that are $\epsilon$ -dependent are evaluated at $\epsilon = 4$.[17] In fact, $\epsilon = 4$ is required in the $\epsilon$ -*RNG* to recover the Kolmogorov energy spectrum in the inertial range.[17] This not only plays some havoc with the evaluation of constants, it also leads to another problem: *RNG*-induced interactions that can be shown to be irrelevant in the limit $\epsilon \ll 1$ cannot now be shown to be irrelevant in the limit $\epsilon \to 4$. Yet in $\epsilon$ -*RNG* theories (which require $\epsilon \to 4$) these higher order nonlinearities are *assumed* to be unimportant.[6,12,16] Moreover, $\epsilon$ - *RNG* theory can only take into account non-local interactions.[6,10,16] However, the procedure is quite amenable and Rubinstein and Barton[7] have derived a Reynolds stress model using $\epsilon$ -RNG methods that is qualitatively similar to that of Speziale[3] and Yoshizawa.[4]

On the other hand, recursion-*RNG* does not rely on an $\epsilon$ -expansion, and treats explicitly the cubic nonlinearities induced into the renormalized momentum equation. Moreover, recursion-*RNG* can handle both local and non-local interactions. Effects such as the cusp behavior in the transport coefficients as $k \to k_c$ are recovered in these theories (here, $k_c$ is the cutoff wavenumber separating the large scale from the local resolvable scales).[13,19-24] These effects are the consequences of local interactions and the cubic nonlinearities introduced by the *RNG* procedure. However, one of the major difficulties to the application of recursion-*RNG* for turbulent flows governed by the Navier-Stokes equation was that the eddy viscosity was determined as a fixed point of a very complicated integro-difference equation. This drawback has now been removed by extending the theory to handle the iterative removal of infinitesimal wavenumber bands.[25] Now, as in $\epsilon$ -*RNG*, the eddy viscosity is readily determined from the solution of a relatively simple differential equation. Unlike $\epsilon$ -*RNG*, though, the transport coefficients are determined over the whole resolvable scales and not just in the wavenumber limit $k \to 0$.

In the present work, the recursion *RNG* procedure is used to develope a Reynolds stress closure model in a formal manner. It is shown that the recursion-*RNG* based model introduces two additional terms arising from the local interactions effects that are of higher order than those obtained using the $\epsilon$ -*RNG* method by considering only the long wavelength, non-local interaction limit. The first of these two terms as well as those from the conventional turbulence models are shown to be a part of the integrity basis used in the representation of the anisotropic part of the Reynolds stress tensor.[26-28] The second term which arises from pressure-strain coupling is quartic in strain rate and is of the same order as the remaining terms of the integrity basis.

The model is then applied for turbulent flow past a backward-facing step which has played a central role in benchmarking the performance of turbulence models for separated flows. During the

past decade — beginning with the 1980/81 Stanford conference on complex turbulent flows[29] — various two-equation turbulence models have been tested and compared with the experimental data of Kim, Kline and Johnston[30] and Eaton and Johnston[31] for the backstep problem. Initial results[29] indicated that the standard $K$-$\varepsilon$ model, with wall functions, underpredicted the reattachment point by a substantial amount on the order of 20-25%. Several independent studies have been subsequently published using alternative forms of the $K$-$\varepsilon$ model wherein a variety of conflicting results have been reported. Considering the need to accurately predict separated turbulent flows — which can have a wealth of important scientific and engineering applications — the proposed model is applied for the backstep problem. The computations based on a sufficiently resolved finite-volume algorithm show that the proposed model based on the recursive application of the renormalization group theory (developed independently without any *ad hoc* empiricism) can yield a prediction for the reattachment point that is within a few percent of the experimental result. The physical implications that these results have will be also discussed in detail in the sections to follow.

## 2. FORMULATION OF THE PHYSICAL PROBLEM

The turbulent motion of viscous, incompressible fluids are governed by the Navier-Stokes equations which may be analyzed using classical single point closure based on Reynolds decomposition of all physical variables. The resulting averaged equations of motion are of the form

$$\frac{\partial U_i}{\partial t} + U_\alpha \frac{\partial U_i}{\partial x_\alpha} = -\frac{\partial P}{\partial x_i} + \nu_0 \frac{\partial^2 U_i}{\partial x_\alpha \partial x_\alpha} - \frac{\partial \tau_{i\alpha}}{\partial x_\alpha} \tag{1}$$

$$\frac{\partial U_\alpha}{\partial x_\alpha} = 0 \tag{2}$$

where $U_i$ is the mean velocity, $P$ is the mean pressure, $\nu_0$ is the kinematic viscosity of the fluid and $\tau_{ij}$ is the Reynolds stress tensor. While the physical aspects of turbulent flows are best described by the above equations, limitations in computer capacity and speed preclude their direct solution for complex flows of engineering importance. The current practice for high Reynolds number flows of engineering interest therefore involves some type of modeling for Reynolds stresses. The commonly used turbulence models are based on the calculation of one-point first and second moments such as the mean velocity, mean pressure and turbulent kinetic energy.

In the present work we consider the development of Reynolds stress model by the recursion *RNG* formulation and its application. In this context it is convenient to express the equations of motion using the Fourier representation,

$$(\frac{\partial}{\partial t} + \nu_0 k^2) u_i(\mathbf{k}, t) = M_{i\alpha\beta}(k) \int d^3p \; u_\alpha(\mathbf{p}, t) u_\beta(\mathbf{k} - \mathbf{p}, t) \tag{3}$$

$$k_\alpha u_\alpha(\mathbf{k}, t) = 0 \tag{4}$$

It is important to note here that *no* random forcing is introduced unlike in the $\in$ -*RNG* theories where it plays a critical role in introducing the small parameter $\in$ . The nonlinear coupling coefficient

$$M_{i\alpha\beta}(k) = k_\beta D_{i\alpha}(k) + k_\alpha D_{i\beta}(k) \tag{5}$$

with $D_{\alpha\beta}$ being the projection operator defined by

$$D_{\alpha\beta}(k) = \delta_{\alpha\beta} - \frac{k_\alpha k_\beta}{k^2} \tag{6}$$

A scale factor $h$ is now introduced to partition the wavenumber space to $N$ segments such that

$$k_c = k_N = h^N k_0 \, ,$$
$$k_{N-1} = h^{N-1} k_0 \, , \quad \ldots \, , \quad k_1 = h k_0 \tag{7}$$
$$k_0 = O(k_d)$$

where, $k_c$ is the cut-off wavenumber that separates the large scale from the small scale, and $k_d$ is of the order of Kolmogorov dissipation wavenumber. The velocity field is then decomposed in the Fourier space such that $u_i = u_i^> \theta (k - k_h) + u_i^< \theta (k_h - k)$ (wherein $\theta$ is the Heavyside unit step function, $k_{h\,(h=1,N)}$ is the local cut-off wavenumber, the superscript $<$ represents large resolvable scale quantities while $>$ represents small unresolved scales with respect to the local cut-off wave-number). The evolution of these components can be directly obtained from (3) as:

$$(\frac{\partial}{\partial t} + \nu_0 k^2) \, u_i^> \, (\mathbf{k}, t) = M_{i\alpha\beta} \, (k) \int d^3 p \, [u_\alpha^< \, (\mathbf{p}, t) \, u_\beta^< \, (\mathbf{k} - \mathbf{p}, t)$$
$$+ 2 u_\alpha^> \, (\mathbf{p}, t) \, u_\beta^< \, (\mathbf{k} - \mathbf{p}, t) + u_\alpha^> \, (\mathbf{p}, t) \, u_\beta^> \, (\mathbf{k} - \mathbf{p}, t)] \tag{8}$$

$$(\frac{\partial}{\partial t} + \nu_0 k^2) \, u_i^< \, (\mathbf{k}, t) = M_{i\alpha\beta} \, (k) \int d^3 p \, [u_\alpha^< \, (\mathbf{p}, t) \, u_\beta^< \, (\mathbf{k} - \mathbf{p}, t)$$
$$+ 2 u_\alpha^> \, (\mathbf{p}, t) \, u_\beta^< \, (\mathbf{k} - \mathbf{p}, t) + u_\alpha^> \, (\mathbf{p}, t) \, u_\beta^> \, (\mathbf{k} - \mathbf{p}, t)] \tag{9}$$

It should be noted that in $\epsilon$-*RNG* approach, one is forced into taking the large-scale infrared limit $k \to 0$. In essence, this forces a spectral gap between the resolvable part of the flow field and the small unresolved scales. If this spectral gap were somehow present initially, it would be quickly populated in just a few eddy turn over times. Thus, retaining only the distant interactions may not be appropriate. In fact, it has been shown[13] that the energy transfer function that corresponds to local interactions accounts for most of the energy flow out of the resolvable scales. It thus seems important to retain both local and nonlocal interactions in the modeling of the Reynolds stress and this can be readily achieved by recursion-*RNG*. In particular, it is apparent that the Reynolds stress, $\tau_{ij} = \tau_{ij}^{>>} + \tau_{ij}^{><}$, has two components. The $\tau_{ij}^{>>}$ – part arises from the infrared limit of $k \to 0$ and is due to the $u_i^> - u_i^>$ distant interaction limit while the $\tau_{ij}^{><}$ – part arises from the $0 < k \leq k_c$ spectrum and is due to the $u_i^> - u_i^<$ local interaction limit. Thus in the $\epsilon$-*RNG* model, the Reynolds stress $\tau_{ij} = \tau_{ij}^{>>}$ and is obtained purely from the $u_i^> - u_i^>$ interaction in the small unresolved scale momentum equation (8). We now consider the contribution to the Reynolds stress that arises from the local interaction:

$$\tau_{ij}^{><} = -\int d^3 p \, [u_i^< \, (\mathbf{k} - \mathbf{p}) \, u_j^> \, (\mathbf{p}) + u_j^< \, (\mathbf{k} - \mathbf{p}) \, u_i^> \, (\mathbf{p})] \tag{10}$$

Herein $\mathbf{u}^<(\mathbf{k}-\mathbf{p})$ corresponds to the Fourier-transformed velocity field in the resolvable large scales, $|\mathbf{k}-\mathbf{p}| < k_1$, while $\mathbf{u}^>(\mathbf{p})$ corresponds to the small scale field with $|\mathbf{p}| > k_1$ and $k_1$ is the wavenumber

which separates the resolvable from the small unresolved scales.

Now there are certain constraints that $\tau_{ij}^{><}$ must satisfy; in particular,

(a) $\tau_{ij}^{><} \to 0$ as the turbulent-kinetic energy $K \to 0$.

(b) $\tau_{ij}^{><}$ is Galilean invariant.

Constraint (a) is clear: as the turbulent kinetic energy $K \to 0$, the small scale velocity field $\mathbf{u}^> \to 0$, so that $\tau_{ij}^{><} \to 0$. Constraint (b) arises since it has been shown in detail that recursion-*RNG*, even with its cubic nonlinearity interaction, is a Galilean invariant theory.[25] Now, if one follows standard recursion-*RNG* procedures,[10-13] the relevant part of the small scale velocity field that contributes to $\tau_{ij}^{><}$ is (on the removal of the first subgrid shell, c.f., equation (9)).

$$u_i^> (\mathbf{p}) = \frac{M_{i\alpha\beta}(p)}{v_0 p^2} \int d^3 j \; u_\alpha^< (\mathbf{j}) \, u_\beta^< (\mathbf{j} - \mathbf{p}) + \dots \tag{11}$$

where, ... refers to terms that will not contribute to $\tau_{ij}^{><}$. At the removal of the first small scale shell $v_0$ is the molecular viscosity. At subsequent steps in the removal of the subgrid scales, $v_0$ will be replaced by the renormalized eddy viscosity.

In the substitution of the subgrid velocity field from (11), into the Reynolds stress $\tau_{ij}^{><}$ given by (10), one must ensure that the constraints, (a) and (b) above are satisfied. It can be shown that these constraints are not satisfied by a simple substitution of (11) into (10). Hence we introduce a factor $(p-k)_\alpha (p-s)_\alpha / k_c^2$ so as to recover these properties. This factor is appropriate since, from (11), $k_c = O(\varepsilon/K^{3/2}) \to \infty$ as $K \to 0$. Hence, in recursion-*RNG*, after the elimination of the first spectral band (i.e., after the first iteration) (10) becomes

$$\tau_{ij}^{><} (\mathbf{k}) \big|_1 = -\frac{1}{k_c^2} \left[ \int d^3 p \, d^3 s \frac{(p_\alpha - k_\alpha)(p_\alpha - s_\alpha)}{v_0 p^2} M_{j\gamma\delta}(p) \, u_\gamma^< (s) \, u_\delta^< (p-s) \, u_i^< (k-p) + i \leftrightarrow j \right] \tag{12}$$

where $p$ is in the subgrid region, while the arguments of all the velocity fields are in the resolvable scales. The second term in (12) is obtained by $i \leftrightarrow j$ interchange in the first term. At the next application of the above procedure (i.e., after the second iteration)

$$\tau_{ij}^{><} (\mathbf{k}) \big|_2 = \tau_{ij}^{><} (\mathbf{k}) \big|_1 - \int d^3 p \, [u_i^< (\mathbf{k} - \mathbf{p}) \, u_j^> (\mathbf{p}) + u_j^< (\mathbf{k} - \mathbf{p}) \, u_i^> (\mathbf{p})] \tag{13}$$

where, $k < k_2$. For $k_2 < k < k_1$, the small scales are obtained by a similar procedure by utilizing the equations of motion for small scales.[10,15] The resulting expression for the small scales may then be written as:

$$u_i^> (\mathbf{p}) = \frac{M_{i\alpha\beta}(p)}{v_1(p) p^2} \int d^3 j \; u_\alpha^< (\mathbf{j}) \, u_\beta^< (\mathbf{j} - \mathbf{p}) + \dots \tag{14}$$

substituting from (12) and (14) in (13),

$$\tau_{ij}^{><}(k) = -\frac{1}{k_c^2}\sum_{h=1}^{2}\left[\int d^3p d^3s \frac{(p_\alpha - k_\alpha)(p_\alpha - s_\alpha)}{v_h(p)p^2}M_{j\gamma\delta}(p)u_\gamma^<(s)u_\delta^<(p-s)u_i^<(k-p) + i\leftrightarrow j\right]$$

(15)

Proceeding similarly to the elimination of the $N$-th spectral band, one finds

$$\tau_{ij}^{><}(k) = -\frac{1}{k_c^2}\sum_{h=1}^{N}\left[\int d^3p d^3s \frac{(p_\alpha - k_\alpha)(p_\alpha - s_\alpha)}{v_h(p)p^2}M_{j\gamma\delta}(p)u_\gamma^<(s)u_\delta^<(p-s)u_i^<(k-p) + i\leftrightarrow j\right]$$

(16)

where, $k_c$ is the cut-off wavenumber that separates the large scales from the small scales. In (16) the summation is over all the spectral bands eliminated and $v_h(p)$ is the renormalized eddy viscosity.[10-13] We now proceed to the differential limit of infinitesimal spectral shells, so that[15]

$$\sum_h v_h(p) \rightarrow \frac{1}{v(k_c)}\left[\frac{p}{k_c}\right]^{4/3}$$

(17)

for a Kolmogorov $k^{-5/3}$ inertial range energy spectrum. Since the quadratic coupling coefficient

$$M_{j\gamma\delta}(p) = \frac{1}{2i}\left(\delta_{j\gamma}p_\delta + \delta_{j\delta}p_\gamma - 2\frac{p_j p_\gamma p_\delta}{p^2}\right)$$

(18)

in the differential limit for infinitesimal spectral shells of the small scales, (16) becomes

$$\tau_{ij}^{><}(k) = -\frac{1}{2iv(k_c)k_c^{10/3}}\left[\int d^3p d^3s \frac{(p_\alpha - k_\alpha)(p_\alpha - s_\alpha)}{p^{2/3}}\{p_\beta u_j^<(s)u_\beta^<(p-s)u_i^<(k-p)\right.$$

$$\left. + p_\beta u_\beta^<(s)u_j^<(p-s)u_i^<(k-p) - 2\frac{p_\beta p_j p_\gamma}{p^2}u_\beta^<(s)u_\gamma^<(p-s)u_i^<(k-p)\} + i\leftrightarrow j\right]$$

(19)

The inverse transform of (19) yields the contribution to Reynolds stress due to local interaction in physical space and is shown below.

$$\tau_{ij}^{><}(x) = \frac{1}{(2\pi)^3 v(k_c)k_c^{10/3}}\left[\frac{\partial U_i(x)}{\partial x_\alpha}\int d^3x'\left(g_1(x-x')\frac{\partial U_j(x')}{\partial x'_\beta}\frac{\partial U_\beta(x')}{\partial x'_\alpha}\right.\right.$$

$$\left.\left. + g_2(x-x')\frac{\partial}{\partial x'_j}\left(\frac{\partial U_\gamma(x')}{\partial x'_\beta}\frac{\partial^2 U_\beta(x')}{\partial x'_\alpha \partial x'_\gamma}\right)\} + i\leftrightarrow j\right]\right.$$

(20)

In the above, the resolvable velocity field in the physical space is identified with the mean velocity $U_i$, and the nonlocal kernels $g_1(x - x')$ and $g_2(x - x')$ are defined by:

$$g_1(\mathbf{r}) = \int \frac{exp\,(i\mathbf{p}\cdot\mathbf{r})}{p^{2/3}}\,d^3p \qquad \text{and} \qquad g_2(\mathbf{r}) = \int \frac{exp\,(i\mathbf{p}\cdot\mathbf{r})}{p^{8/3}}\,d^3p \qquad (21)$$

The structure of these nonlocal kernels is dependent on the cut-off wavenumber, $k_c$. Now,

$$g_1(r) = \frac{4\pi}{r} \int_{k_c}^{2k_c} p^{1/3} \sin\,(pr)\,dp = \frac{4\pi}{r} k_c^{4/3} \int_1^2 p'^{1/3} \sin\,(k_c p' r)\,dp' \qquad (22)$$

where the integration limits are obtained from the partial average[15] over the nearest unresolved band. Similarly,

$$g_2(r) = \frac{4\pi}{r} k_c^{-2/3} \int_1^2 p'^{-5/3} \sin\,(k_c p' r)\,dp'. \qquad (23)$$

These nonlocal kernels reduce to local expressions for $k_c \gg 1$. Noting that $\sin\,(k_c x)\,/x \to \pi\delta\,(x)$ as $k_c \to \infty$,

$$g_1(r)\,/4\pi \approx 3.58 k_c^{4/3}\delta\,(r)$$

$$g_2(r)\,/4\pi \approx 1.74 k_c^{-2/3}\delta\,(r). \qquad (24)$$

Following Yakhot and Orszag,[5] this cutoff wavenumber $k_c$ can be related to the isotropic part of the turbulent kinetic energy $K$ as:

$$K = \int_{k_c}^{\infty} E\,(p)\,dp = \frac{3}{2} C_K \frac{\varepsilon^{2/3}}{k_c^{2/3}} \qquad (25)$$

on using the Kolmogorov intertial range spectrum for $E(p)$, and where $C_K$ is the Kolmogorov constant. Thus, the cut-off wavenumber

$$k_c = \frac{\varepsilon}{K^{3/2}} (\frac{3}{2} C_K)^{3/2}. \qquad (25)$$

Hence under this approximation $\tau_{ij}^{><}(\mathbf{x})$ in (20) reduces to a simple algebraic form

$$\tau_{ij}^{><}(\mathbf{x}) = C_{R1} \frac{K^4}{\varepsilon^3} \left[ \frac{\partial U_i}{\partial x_\alpha} \frac{\partial U_j}{\partial x_\beta} \frac{\partial U_\beta}{\partial x_\alpha} + i \leftrightarrow j \right] + C_{R2} \frac{K^7}{\varepsilon^5} \left[ \frac{\partial U_i}{\partial x_\alpha} \frac{\partial}{\partial x_j} \left( \frac{\partial U_\beta}{\partial x_\gamma} \frac{\partial^2 U_\gamma}{\partial x_\alpha \partial x_\beta} \right) + i \leftrightarrow j \right] \qquad (27)$$

where use has been made of Kraichnan's[32] result

$$\nu\,(k_c)\,k_c^{4/3} = 0.19 C_K^2 \varepsilon^{1/3} \qquad (28)$$

- 8 -

However, for most flows of interest, $k_c$ varies considerably throughout the flow domain. Thus, if one wishes to use the local approximation for the kernels, $g_1$ and $g_2$ as well as retain $k_c \sim O(1)$ effects so as to obtain an algebraic form for $\tau_{ij}^{><}(\mathbf{x})$, then the coefficients $C_{R1}$ and $C_{R2}$ will be function of the flow quantities. In particular, $C_{R1}$ and $C_{R2}$ may be expressed as:

$$C_{R1} = C_{R1}(\varepsilon, K, \eta, \zeta) \qquad \text{and} \qquad C_{R2} = C_{R2}(\varepsilon, K, \eta, \zeta) \qquad (29)$$

where

the strain rate, $\eta \equiv (S_{\alpha\beta}S_{\alpha\beta})^{1/2}$, with $S_{\alpha\beta} \equiv \dfrac{1}{2}\left(\dfrac{\partial U_\alpha}{\partial x_\beta} + \dfrac{\partial U_\beta}{\partial x_\alpha}\right)$ and

the rotation rate, $\zeta \equiv (W_{\alpha\beta}W_{\alpha\beta})^{1/2}$, with $W_{\alpha\beta} \equiv \dfrac{1}{2}\left(\dfrac{\partial U_\alpha}{\partial x_\beta} - \dfrac{\partial U_\beta}{\partial x_\alpha}\right)$.

Rubinstein and Barton[7] have derived a Reynolds stress model using the $\epsilon$-$RNG$ method (which corresponds to the infrared limit of $k \to 0$) of the following form:

$$
\tau_{ij}^{>>} = -\frac{2}{3}K\delta_{ij} + \nu_T\left(\frac{\partial U_i}{\partial x_j} + \frac{\partial U_j}{\partial x_i}\right) - \frac{K^3}{\varepsilon^2}\left[C_{\tau1}\left(\frac{\partial U_i}{\partial x_\alpha}\frac{\partial U_j}{\partial x_\alpha}\right)^*\right.
$$
$$
\left. + C_{\tau2}\left(\frac{\partial U_i}{\partial x_\alpha}\frac{\partial U_\alpha}{\partial x_j} + \frac{\partial U_j}{\partial x_\alpha}\frac{\partial U_\alpha}{\partial x_i}\right)^* + C_{\tau3}\left(\frac{\partial U_\alpha}{\partial x_i}\frac{\partial U_\alpha}{\partial x_j}\right)^*\right] \qquad (30)
$$

The constants $C_{\tau1} = 0.034$, $C_{\tau2} = 0.104$ and $C_{\tau3} = -0.014$, and $(\ldots)^*$ denotes the deviatoric part of the expression within the parenthesis. The first two terms correspond to the linear model and $\nu_T = C_\mu K^2/\varepsilon$ is the isotropic eddy-viscosity, where $\varepsilon$ is the turbulence dissipation and $C_\mu \approx 0.09$ based on empirical data from equilibrium boundary layer flows. The above model is quadratic in mean strain rate, includes the effect of convection and diffusion and is qualitatively similar to other second order models.[3,4]

Combining (27) – (30) a formal expression for Reynolds stress which includes both the local and nonlocal interactions may be expressed in the following form:

$$
\tau_{ij} = -\frac{2}{3}K\delta_{ij} + \nu_T\left(\frac{\partial U_i}{\partial x_j} + \frac{\partial U_j}{\partial x_i}\right) - \frac{K^3}{\varepsilon^2}\left[C_{\tau1}\left(\frac{\partial U_i}{\partial x_\alpha}\frac{\partial U_j}{\partial x_\alpha}\right)^*\right.
$$
$$
\left. + C_{\tau2}\left(\frac{\partial U_i}{\partial x_\alpha}\frac{\partial U_\alpha}{\partial x_j} + \frac{\partial U_j}{\partial x_\alpha}\frac{\partial U_\alpha}{\partial x_i}\right)^* + C_{\tau3}\left(\frac{\partial U_\alpha}{\partial x_i}\frac{\partial U_\alpha}{\partial x_j}\right)^*\right]
$$
$$
+ C_{R1}\frac{K^4}{\varepsilon^3}\left[\frac{\partial U_i}{\partial x_\alpha}\frac{\partial U_j}{\partial x_\beta}\frac{\partial U_\beta}{\partial x_\alpha} + i \leftrightarrow j\right] + C_{R2}\frac{K^7}{\varepsilon^5}\left[\frac{\partial U_i}{\partial x_\alpha}\frac{\partial}{\partial x_j}\left(\frac{\partial U_\beta}{\partial x_\gamma}\frac{\partial^2 U_\gamma}{\partial x_\alpha \partial x_\beta}\right) + i \leftrightarrow j\right] \qquad (31)
$$

It is of some interest to recast the above expression for the Reynolds stress obtained from the recursion *RNG* model into an integrity basis representation which are commonly employed to represent the anisotropic part of the Reynolds stress tensor, $b_{ij} = (\tau_{ij} - \frac{2}{3} K \delta_{ij}) / 2K$ in the following form-invariant manner.[26-28]

$$b_{ij} = \sum_{\lambda} G^{(\lambda)} T_{ij}^{(\lambda)} \tag{32}$$

where, $T_{ij}^{(\lambda)}$ is the integrity basis for functions of symmetric and antisymmetric tensor and the coefficients $G^{(\lambda)}$ are scalar functions of the irreducible invariants of the strain rate tensor, $S_{ij}$ and the rotation rate tensor, $W_{ij}$.[26-28]

$$T_{ij}^{(1)} = S_{ij}$$

$$T_{ij}^{(2)} = S_{i\alpha} W_{\alpha j} - W_{i\alpha} S_{\alpha j}$$

$$T_{ij}^{(3)} = S_{i\alpha} S_{\alpha j} - \frac{1}{3} S_{\alpha\alpha} \delta_{ij}$$

$$T_{ij}^{(4)} = W_{i\alpha} W_{\alpha j} - \frac{1}{3} W_{\alpha\alpha} \delta_{ij}$$

$$T_{ij}^{(5)} = W_{i\alpha} S_{\alpha\beta} S_{\beta j} - S_{i\alpha} S_{\alpha\beta} W_{\beta j}$$

$$T_{ij}^{(6)} = W_{i\alpha} W_{\alpha\beta} S_{\beta j} + S_{i\alpha} W_{\alpha\beta} W_{\beta j} - \frac{2}{3} (S_{\alpha\beta} W_{\beta\gamma} W_{\gamma\alpha}) \delta_{\alpha\beta}$$

$$T_{ij}^{(7)} = W_{i\alpha} S_{\alpha\beta} W_{\beta\gamma} W_{\gamma j} - W_{i\alpha} W_{\alpha\beta} S_{\beta\gamma} W_{\gamma j}$$

$$T_{ij}^{(8)} = S_{i\alpha} W_{\alpha\beta} S_{\beta\gamma} S_{\gamma j} - S_{i\alpha} S_{\alpha\beta} W_{\beta\gamma} S_{\gamma j}$$

$$T_{ij}^{(9)} = W_{i\alpha} W_{\alpha\beta} S_{\beta\gamma} S_{\gamma j} + S_{i\alpha} S_{\alpha\beta} W_{\beta\gamma} W_{\gamma j} - \frac{2}{3} (S_{\alpha\beta} S_{\beta\gamma} W_{\gamma\epsilon} W_{\epsilon\alpha}) \delta_{ij}$$

$$T_{ij}^{(10)} = W_{i\alpha} S_{\alpha\beta} S_{\beta\gamma} W_{\gamma\epsilon} W_{\epsilon j} - W_{i\alpha} W_{\alpha\beta} S_{\beta\gamma} S_{\gamma\epsilon} W_{\epsilon j} \tag{33}$$

Recently, Gatski and Speziale[28] have applied this integrity basis to determine an explicit algebraic stress model for three dimensional turbulent flows based on a systematic derivation from a hierarchy of second-order closure models. In their applications, they have restricted themselves to a model[28] which involves just the tensors $T_{ij}^{(1)}$, $T_{ij}^{(2)}$, and $T_{ij}^{(3)}$. It can readily be shown that the $k = 0$ part of the Reynolds stress, $\tau_{ij}^{>>}$, specified in (30), involves the tensors $T_{ij}^{(1)}$, $T_{ij}^{(2)}$, $T_{ij}^{(3)}$ and $T_{ij}^{(4)}$ from the integrity basis given by (33). The $\tau_{ij}^{>>}$-part of the Reynolds stress is common to both $\epsilon$-RNG and recursion-RNG. However, unlike $\epsilon$-*RNG*, there is now a finite-$k$ spectral contribution, $\tau_{ij}^{><}$ to the Reynolds stress in recursion-*RNG*. It can be shown that the first term in (29) involves the tensors $T_{ij}^{(5)}$ and $T_{ij}^{(6)}$ of the integrity basis (33). The second term in (29), however, is not readily expressed in this second order basis because of the intrinsic fourth rank tensors involved.

However, as can be seen, this term is quartic in strain rate and arises from pressure-strain coupling, and could be thought of as having contributions similar to those involving the tensors $T_{ij}^{(7)}$, $T_{ij}^{(8)}$, and $T_{ij}^{(9)}$.

The above expression for Reynolds stress (31) are to be used along with the equations of motion (1) by specifying turbulent kinetic energy and dissipation. In two-equation turbulence models, this closure is achieved through the development of transport equations for the turbulent kinetic energy and dissipation — quantities that are directly related to the length and time scales — of the following general form:

$$\frac{\partial K}{\partial t} + U_j \frac{\partial K}{\partial x_j} = \mathcal{P} - \varepsilon + \frac{\partial}{\partial x_i}\left[\left(\nu_0 + \frac{\nu_T}{\alpha_K}\right)\frac{\partial K}{\partial x_i}\right] \tag{34}$$

$$\frac{\partial \varepsilon}{\partial t} + U_j \frac{\partial \varepsilon}{\partial x_j} = C_{\varepsilon 1}\frac{\varepsilon}{K}\mathcal{P} - C_{\varepsilon 2}\frac{\varepsilon^2}{K} + \frac{\partial}{\partial x_i}\left[\left(\nu_0 + \frac{\nu_T}{\alpha_\varepsilon}\right)\frac{\partial \varepsilon}{\partial x_i}\right] - \mathcal{R} \tag{35}$$

where, $\nu = \nu_0 + \nu_T$ is the total viscosity, $\mathcal{P} = -\tau_{ij}(\partial U_i/\partial x_j)$ is the turbulence production, $\varepsilon$ is the scalar turbulent dissipation rate, and $\mathcal{R} = 2\nu_0 S_{ij}\overline{(\partial u_j/\partial x_i)\,(\partial u_i/\partial x_j)}$ is the turbulent strain rate correlation term. The quantities $C_{\varepsilon 1}$, $C_{\varepsilon 2}$, $\alpha_K$, $\alpha_\varepsilon$ are dimensionless and taken to be 1.44, 1.92, 1.0 and 1.3, respectively, consistent with the standard form of the two-equation $K-\varepsilon$ model (based on empirical data obtained from equilibrium boundary layer flows).[4] It should be noted here that these are calculated explicitly to be 1.42, 1.68, 0.719 and 0.719, respectively, in the $\varepsilon$-RNG-based formulations.[5,6] In addition, it is customary to neglect the strain rate correlation term $\mathcal{R}$ in the standard $K-\varepsilon$ model as well as in some RNG-based models[7] since $\mathcal{R}$ must be modeled in order to achieve closure. Special forms of approximations have been recently employed in the case of some of the $\varepsilon$-RNG-based models.[8,9] To avoid ambiguity (and to avoid introducing *ad hoc* assumptions required to model $\mathcal{R}$) the contribution from the turbulent strain rate correlation term is neglected in the present work.

# 3. TURBULENT FLOW PAST A BACKWARD-FACING STEP — A CASE STUDY

The problem to be considered is the fully-developed turbulent flow of an incompressible viscous fluid past a backward-facing step (a schematic is provided in figure 1). Calculations will be conducted for an expansion ratio (step height: outlet channel height) $E$ of 1:3 and the Reynolds number $Re$ = 132,000 based on the inlet centerline mean velocity and outlet channel height (which corresponds to that of Kim et al.[30] and Eaton and Johnston[31]). The mean turbulence equations (cf., §2) are solved subject to the following boundary conditions:[33]

(a) inlet profiles for $U$, $K$ and $\varepsilon$ are specified five step heights upstream of the step corner ($U$ is taken from the experimental data[30,31] and the corresponding profiles for $K$ and $\varepsilon$ are computed from the model formulated for channel flow),

(b) The law of the wall is used at the upper and the lower walls, and

(c) Conservative extrapolated outflow conditions are applied thirty step heights downstream of the step corner; these conditions involve the following: i) the $V$-component of the velocity for the cells at the outflow boundary are obtained by extrapolation; ii) the $U$-component of the velocity is then computed by the application of a mass balance; and iii) the scalar quantities such as pressure, turbulent kinetic energy and turbulent dissipation are all obtained by extrapolation. It was found that a downstream channel length of about thirty step heights was needed to ensure that the local error for all the quantities was of the same order as the interior values.

A finite volume method which relies on solving the discretized equations by a line relaxation method with the repeated application of the tridiagonal matrix solution algorithm is modified and applied for the present case to obtain the steady state solution.[33,34] The computed solution was assumed to have converged to its steady state when the root mean square of the average difference between successive iterations was less than $10^{-4}$ for the mass source.[34] Approximately 2000 iterations were needed for the convergence of the standard $K$-$\varepsilon$ model; this corresponds to approximately 20 minutes of *CPU* time in a partially vectorized mode on the *Cray-YMP* supercomputer using 64-bit precision. The recursive *RNG*-based $K$-$\varepsilon$ model requires approximately 33% more *CPU* time due to the fact that the additional terms in the *RNG*-based $K$-$\varepsilon$ model have to be evaluated during each iteration. These correction terms are dispersive — an additional feature that slows convergence.

The issue of resolution is crucial for the backstep problem and calculations indicate that a 200×100 mesh yields a fully grid independent solution.[33] All of the computations conducted in this study were performed using this 200×100 nonuniform mesh. As indicated earlier, the inlet conditions were specified 5 step heights upstream of the step corner and the outlet boundary conditions were specified 30 step heights downstream of the step corner. It is crucial that a sufficient distance downstream of the reattachment point be allowed before the outflow conditions are imposed. Many

earlier computations of the backstep problem were in significant error due to the imposition of fully-developed outflow conditions too close to the reattachment point. Furthermore, it is crucial that a fine mesh be used near the step corner for computational accuracy. It should be also noted that the law of the wall does not formally apply to separated turbulent boundary layers. However, since the separation point is fixed at the corner of the backstep — and the flowfield is solved iteratively so that the friction velocity $u_\tau$ can be updated until it converges — major errors do not appear to result from its use.[33]

First, results will be presented for the standard $K$-$\varepsilon$ model. For this case — as well as the other results to follow — computed results for the mean velocity streamlines, the streamwise mean velocity profiles, the streamwise turbulence intensity profiles and the turbulence shear stress profiles are compared with the Kim *et al.*[30] experimental data as updated by Eaton and Johnston.[31] In figure 2(a) the computed streamlines are shown, indicating reattachment at $X_r/H \approx 6.12$ — a result which is approximately 15% underprediction of the experimental reattachment point of $X_r/H \approx 7.1$. In figure 2(b), the streamwise mean velocity profiles predicted by the standard $K$-$\varepsilon$ model are compared with the experimental data. Except in the vicinity of the reattachment point, the comparisons are fairly good. More serious discrepancies between the model predictions and the experimental data occur in the initial part of the recovery zone for the streamwise turbulence intensity profiles as shown in figure 3(a). However, the model predictions for the turbulence shear stress profiles are reasonably good as can be seen from figure 3(b).

Next, we consider the computations based on the recursion-*RNG* model. For computational efficiency, the nonlocal kernels $g_1$ and $g_2$ are approximated by one-dimensional delta functions. This is appropriate if $k_c \gg 1$. In Fig. 4, the variation of $k_c$ (normalized by the step height and expressed as $k_cH$) is shown at various locations downstream of the step. As can be seen, the magnitude of $k_c$ is at least an order of magnitude larger than the grid size employed ($k_cH > 1$ for the $200 \times 100$ mesh used). Thus the local representation of $g_1$ and $g_2$ is justified. The explicit functional form of the coefficients $C_{R1}$ and $C_{R2}$, (29), is much more difficult to evaluate. As a first attempt at applying this recursion-*RNG* model we make a lowest order approximation that these coefficients are constants. Clearly, especially in light of the great success in enforcing a functional *ansatz* on these types of coefficients,[9] this will underestimate the robustness and accuracy of the recursion-*RNG* formulation. Nevertheless, it is deemed more appropriate here to apply the theory without adding on these extraneous functional *ansatzes*. It is also evident that in applying the one-dimensional local form of $g_1 (|\mathbf{x} - \mathbf{x'}|)$ and $g_2 (|\mathbf{x} - \mathbf{x'}|)$, the angular dependences of the second term in (22) is much stronger than that of the first term in (22). This is because of the higher order derivatives present. These angular integrations are also dependent on spatial position due to the changing flow characteristics. Again, for simplicity, we approximate these angular integrations by constants, and

thus put the model to an even stricter test. In particular, for the present analysis, $C_{R1}$ and $C_{R2}$ are taken to be 0.025 and 0.0342 × $10^{-3}$, respectively.

Now, it will be demonstrated that the use of the proposed recursive *RNG*-based model can yield a more significant improvement in the results. The computed streamlines for the flow field shown in figure 5(a) have a mean reattachment point, $X_r/H \approx 6.72$, a result which is about 5% lower than the experimental value. The corresponding mean velocity profiles shown in figure 5(b) indicate very good agreement with the experimental results. It should be noted that computations performed based on the $\in$ -*RNG*-based model for the same flow conditions and model constants yield a mean reattachment point, $X_r/H \approx 6.42$ (not shown herein). The difference in the size of the separated flow region can be clearly attributed to the contributions from the Reynolds stress terms representing the local interactions effects in the recursion *RNG* model.

Furthermore the overall agreement between the turbulence intensity and the shear stresses with the experimental data shown in figures 6(a) and 6(b) are also good. The most notable difference between the predictions of the *RNG*-based models and the standard $K$-ε model lies in the stream-wise turbulence intensity (figure 6(a)). The slight trough shaped variation predicted in this region is consistent with more recent independent experiments.[35]

In addition, to illustrate the differences associated with the modeling of the Reynolds stresses, the variation of the turbulent eddy-viscosity normalized with respect to its molecular counterpart, $v_T/v_0$, is shown at several locations downstream of the backward-facing step. As can be seen, in the recirculation region the eddy viscosity predicted by the standard $K$-ε model is generally larger than that due to the recursion *RNG* leading to substantial reduction in the size of the separated flow region (cf., figures 2(a) and 5(a)).

The wall pressure coefficient is an important parameter for engineering applications. In figures 8(a)-(b), the pressure coefficients $C_p$ ($= 2[p - p_r]/U_r^2$, where $p_r$ and $U_r$ are the reference pressure and velocity which are taken at the centerline of the inlet) obtained from the standard and the conventional and the *RNG*-based $K$-ε models at the top and bottom walls are compared with the experimental data of Eaton and Johnston.[31]  As can be seen, both the standard and the *RNG*-based $K$-ε models perform comparably well in reproducing the experimental trends. The skin friction coefficients $C_f = 2u_\tau^2/U_r^2$ obtained from the standard and recursion-*RNG* $K$-ε models are compared with the scaled experimental data of Driver and Seegmiller[36] for the bottom wall in figure 8(c). Here, we make use of the fact that the ratio $C_f/C_{f\infty}$, when taken as a function of the normalized distance $(X-X_r)/X_r$, is independent of the expansion ratio (given that $C_{f\infty}$ is the fully-developed skin friction coefficient and $X_r$ is the reattachment point). As can be seen, the recursive *RNG*-based $K$-ε model performs better, however, both models are probably within the uncertainty of the experimental data.

## 4. CONCLUSIONS

The recursion renormalization group (*RNG*) theory is utilized to develop Reynolds stress closure models for the prediction of turbulent separated flows. Unlike the small parameter $\epsilon$ *-RNG* model that only consider the interaction of the long wavelength modes, the recursion-*RNG* model includes both the local and nonlocal interaction of all the relevant resolvable scales. A formal development of the Reynolds stress model is presented and the resulting higher order terms by consideration of the local interaction effects are shown to be qualitatively similar to those recently obtained by considering a hierarchy of second-order closure models.[26-28]

The ability of the proposed model to accurately predict separated flows is analyzed from a combined theoretical and computational standpoint by considering turbulent flow past a backward facing step as a test case. The results obtained based on detailed computations demonstrate that the proposed recursion–*RNG* model can yield very good predictions for the turbulent flow of an incompressible viscous fluid over a backward-facing step. It should be remembered that the deficiencies of two-equation models are well established, particularly in turbulent flows with body forces or Reynolds stress relaxation effects.[1] Consequently, the findings of this study should not be interpreted as an unequivocal endorsement of two-equation *RNG* models. Nonetheless, this study shows that properly calibrated two-equation turbulence models, which account for the anisotropy of the turbulent stresses, can be effective for the prediction of turbulent separated flows.

## ACKNOWLEDGEMENTS

# REFERENCES

[1] C. G. Speziale, *Ann. Rev. Fluid Mech.*, **23**, 107 (1991)

[2] B. E. Launder and D. B. Spalding, *Comput. Methods Appl. Mech. Eng.*, **3**, 269 (1974)

[3] C. G. Speziale, *J. Fluid Mech.*, **178**, 459 (1987)

[4] A. Yoshizawa, *Phys. Fluids*, **27**, 1377 (1984)

[5] V. Yakhot and S. A. Orszag, *J. Sci. Comput.*, **1**, 3 (1986)

[6] L. M. Smith and W. C. Reynolds, *Phys. Fluids*, **A4**, 364 (1992)

[7] R. Rubinstein and J. M. Barton, *Phys. Fluids*, **A2**, 1472 (1990)

[8] V. Yakhot and L. M. Smith, *J. Sci. Comput.*, **7**, 35 (1992)

[9] V. Yakhot, S. A. Orszag, S. Thangam, T. B. Gatski and C. G. Speziale, *Phys. Fluids*, **A4**, 1510 (1992)

[10] Y. Zhou, G. Vahala and M. Hossain, *Phys. Rev.*, **A37**, 2590 (1988)

[11] Y. Zhou, G. Vahala and M. Hossain, *Phys. Rev.*, **A40**, 5865 (1989)

[12] Y. Zhou and G. Vahala, *Phys. Rev.*, **A46**, 1136 (1992)

[13] Y. Zhou and G. Vahala, *Phys. Rev.*, **E47**, 2503 (1993)

[14] D. Forster, D. Nelson and M. Stephen, *Phys. Rev.*, **A16**, 732 (1977)

[15] H. A. Rose, *J. Fluid Mech.*, **81**, 719 (1977)

[16] R. H. Kraichnan, *Phys. Fluids*, **30**, 2400 (1987)

[17] S. H. Lam, *Phys. Fluids A*, **4**, 1007 (1992)

[18] W. D. McComb, *The Physics of Fluid Turbulence* (Clarendon, Oxford, 1990)

[19] R. H. Kraichnan, *J. Atmos. Sci.*, **33**, 1521 (1976)

[20] D. C. Leslie and G. L. Quarini, *J. Fluid Mech.*, **91**, 65 (1979)

[21] J. P. Chollet and M. Lesieur, *J. Atmos. Sci.*, **38**, 2747 (1981)

[22] J.A. Domaradzski, R. W. Metcalfe, R. S. Rogallo, and J. J. Riley, *Phys. Rev. Lett.*, **58**, 547 (1987)

[23] M. Lesieur and R. Rogallo, *Phys. Fluids A*, **1**, 718 (1989)

[24] J. R. Chasnov, *Phys. Fluids A*, **3**, 188 (1991)

[25] Y. Zhou and G. Vahala, *Phys. Rev.* E (submitted; also available as *ICASE Report 93-1*, 1993)

[26] A. J. M. Spencer, in *Continuum Physics* (ed. A. C. Eringen, Academic Press), **1**, 1 (1971)

[27] S. B. Pope, *J. Fluid Mech.*, **72**, 331 (1975)

[28] T. B. Gatski and C. G. Speziale, *NASA-ICASE Report 92-58* (to appear, *J. Fluid Mech.*, 1993)

[29] S. J. Kline, B. J. Cantwell, and G. M. Lilley, eds., *Proc. of the 1980-81 AFOSR-HTTM Stanford Conference on Complex Turbulent Flows*, Stanford University Press, Stanford, CA (1981)

[30] J. Kim, S. J. Kline, and J. P. Johnston, *ASME J. of Fluids Engineering*, **102**, 302 (1980)

[31] J. Eaton and J. P. Johnston, *Technical Report MD-39*, Stanford University, CA (1980)

[32] R. H. Kraichnan, *J. Fluid Mech.*, **47**, 525 (1971)

[33]S. Thangam and C. G. Speziale, *AIAA Journal*, **30**, 1314 (1992)

[34]D. G. Lilley and D. L. Rhode, "A computer code for swirling turbulent axisymmetric recirculating flows in practical isothermal combustor geometries," *NASA Contractor Report CR-3442* (1982)

[35]J. F. Meyers, S. O. Kjelgaard, and T. E. Hepner, *Fifth International Symposium on Applications of Laser Technologies to Fluid Mechanics*, Lisbon, Portugal, (1990)

[36]D. M. Driver and H. L. Seegmiller, *AIAA Journal*, **23**, 163 (1985)

## LIST OF FIGURES

**Physical Configuration and Coordinate System**
**Figure 1**

Y/H

3

2

1

0

−1    0    5    10

X/H

**(a) Streamlines**

X/H :   1.33      2.67      5.33      6.22      8.00     10.67

3

2

Y
—
H

1

0

0   1    0   1    0   1    0   1    0   1    0   1

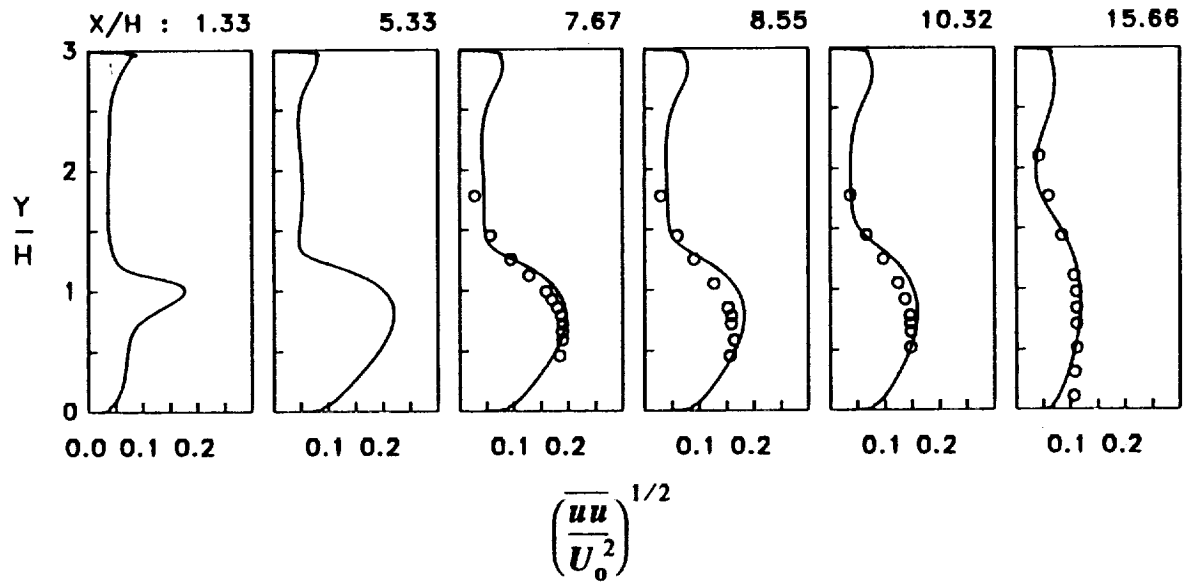$$\frac{\overline{u}}{U_0}$$
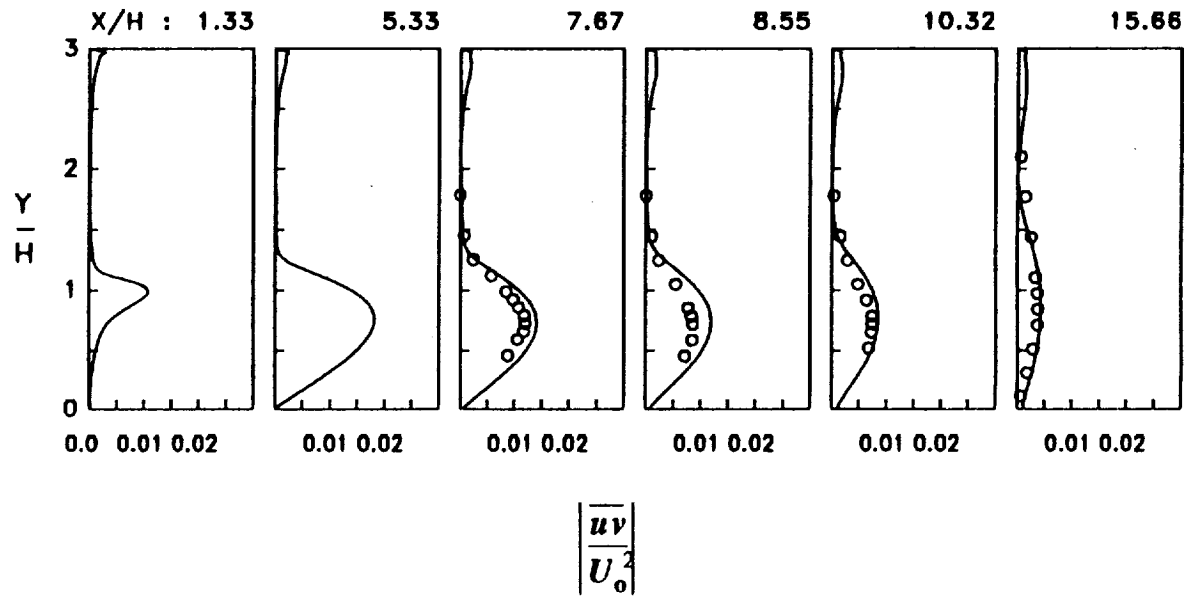
**(b) Dimensionless mean velocity profile**

**(—— Computations;**

**o Experiments of Kim *et al*, 1980; Eaton & Johnston, 1981)**

**Figure 2 Computed mean flow field for the standard *K*-ε model**
**[E = 1:3; Re = 132,000; 200x100 mesh]**

$$\left(\frac{\overline{uu}}{U_o^2}\right)^{1/2}$$

(a) Turbulence Intensity



$$\left|\frac{\overline{uv}}{U_o^2}\right|$$

(b) Turbulence shear stress

Figure 3 Computed turbulence stresses for the standard $K$-$\varepsilon$ model [E = 1:3; Re = 132,000; 200x100 mesh; —— computations; o experiments of Kim *et al*, 1980; Eaton & Johnston, 1981]

X/H : 1.00    2.00    3.00    5.00    8.00    15.00

$k_c H$
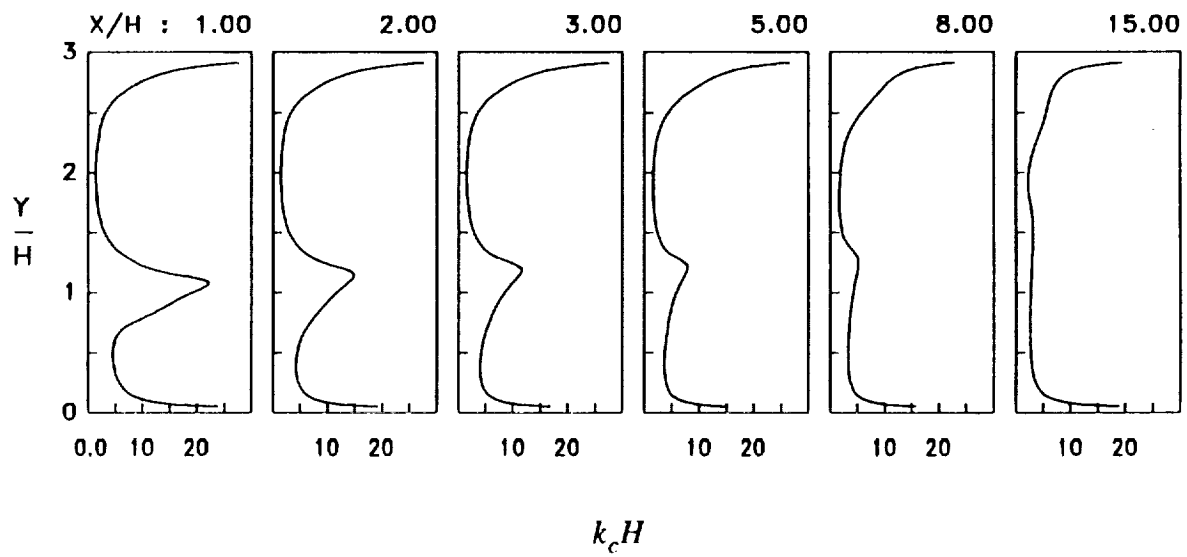
Figure 4   Computed profiles of the cut-off wavenumber for the recursion RNG $K$-$\varepsilon$ model [E = 1:3; Re = 132,000; 200x100 mesh; —— computations; o experiments of Kim *et al*, 1980; Eaton & Johnston, 1981]

**(a) Streamlines**
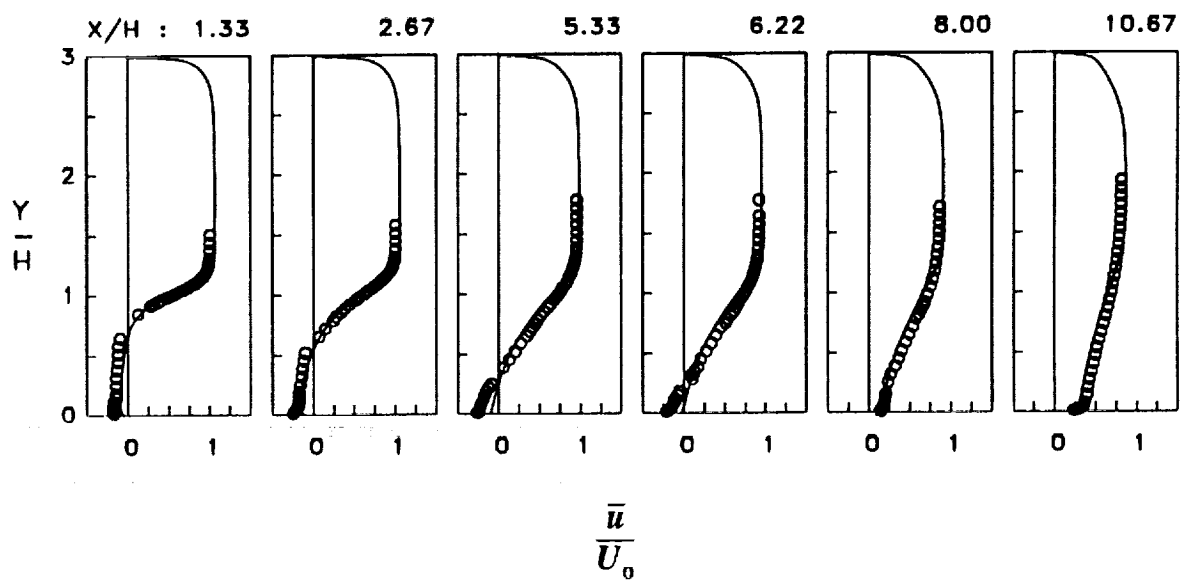


X/H : 1.33        2.67        5.33        6.22        8.00        10.67

$$\frac{\bar{u}}{U_0}$$

**(b) Dimensionless mean velocity profile**

(———— Computations;

o Experiments of Kim *et al*, 1980; Eaton & Johnston, 1981)

**Figure 5 Computed mean flowfield for the recursion RNG *K*-ε model**
**[E = 1:3; Re = 132,000; 200x100 mesh]**

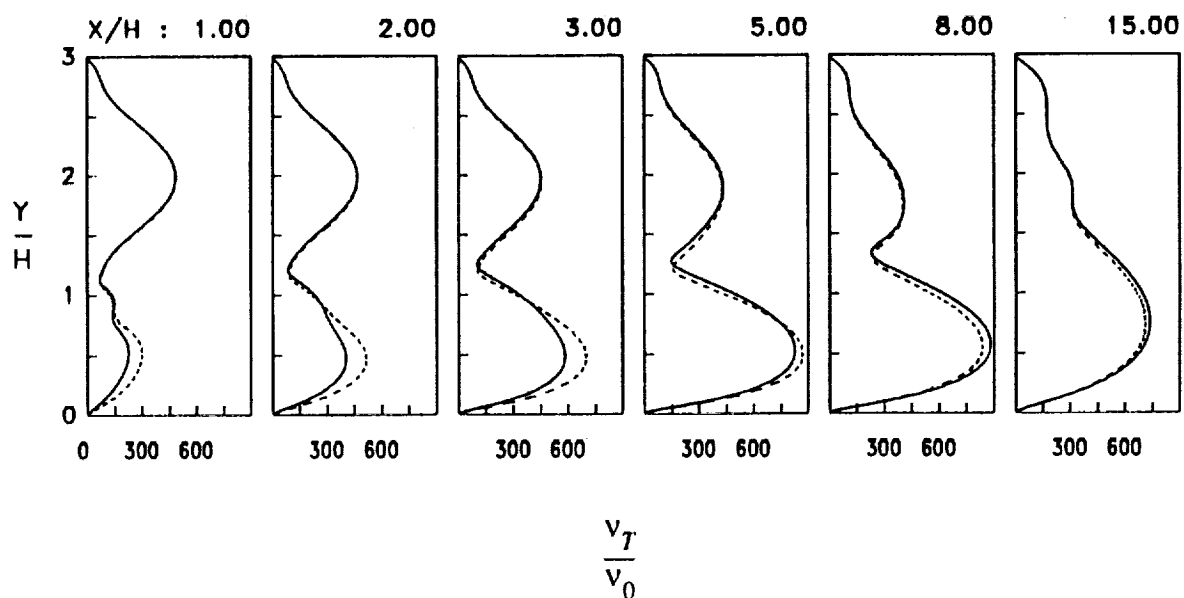$$\left(\frac{\overline{uu}}{U_o^2}\right)^{1/2}$$

(a) Turbulence Intensity



$$\left|\frac{\overline{uv}}{U_o^2}\right|$$

(b) Turbulence shear stress

Figure 6   Computed turbulence stresses for the recursion RNG $K$-$\varepsilon$ model [E = 1:3; Re = 132,000; 200x100 mesh; —— computations; o experiments of Kim *et al*, 1980; Eaton & Johnston, 1981]

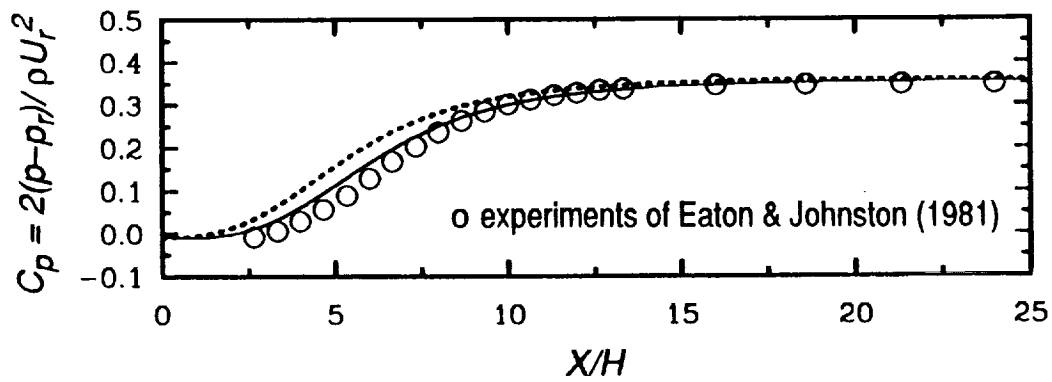X/H : 1.00    2.00    3.00    5.00    8.00    15.00

$$\frac{v_T}{v_0}$$

**Figure 7 Computed profiles of eddy-viscosity [E = 1:3; Re = 132,000; 200x100 mesh; – – – computations for the standard $K$-$\varepsilon$ model; ——— computations for the recursion *RNG* $K$-$\varepsilon$ model]**
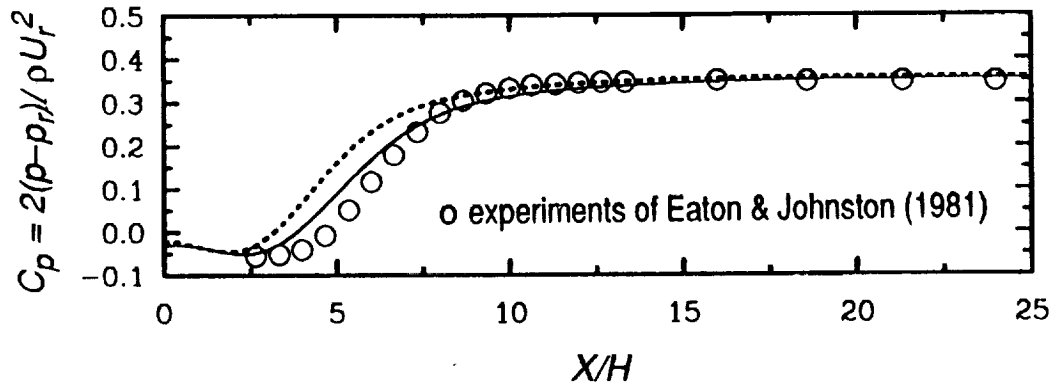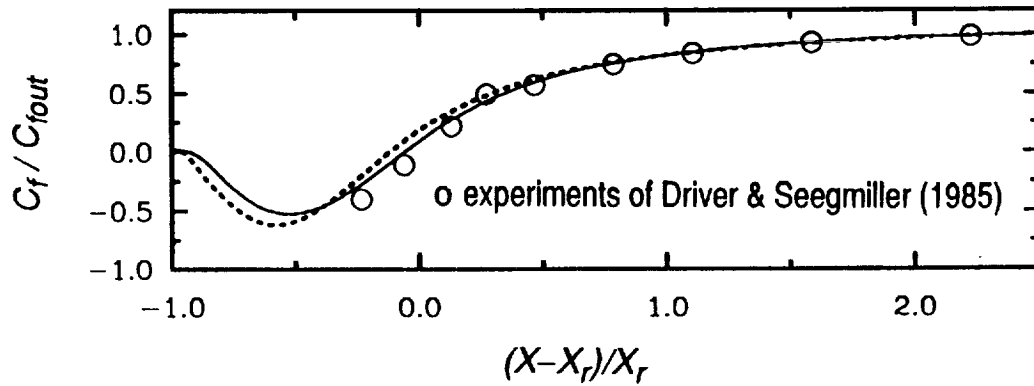
**(a) Pressure coefficient along the bottom wall**



**(b) Pressure coefficient along the top wall**



**(c) Skin friction coefficient along the bottom wall**

Figure 8    Comparison of the predicted wall distribution with experiments
[------ computations for the standard $K$-$\varepsilon$ model; —— computations for the recursion *RNG* $K$-$\varepsilon$ model; o experiments; $E$ = 1:3; *Re* = 132,000]

# REPORT DOCUMENTATION PAGE

| 1. AGENCY USE ONLY (Leave blank) | 2. REPORT DATE<br>August 1993 | 3. REPORT TYPE AND DATES COVERED<br>Contractor Report |
|---|---|---|

**4. TITLE AND SUBTITLE**

DEVELOPMENT OF A RECURSION RNG-BASED TURBULENCE MODEL

**6. AUTHOR(S)**

Ye Zhou, George Vahala, and S. Thangam

**5. FUNDING NUMBERS**

C NAS1-19480

WU 505-90-52-01

**7. PERFORMING ORGANIZATION NAME(S) AND ADDRESS(ES)**

Institute for Computer Applications in Science
and Engineering
Mail Stop 132C, NASA Langley Research Center
Hampton, VA 23681-0001

**8. PERFORMING ORGANIZATION REPORT NUMBER**

ICASE Report No. 93-51

**9. SPONSORING/MONITORING AGENCY NAME(S) AND ADDRESS(ES)**

National Aeronautics and Space Administration
Langley Research Center
Hampton, VA 23681-0001

**10. SPONSORING/MONITORING AGENCY REPORT NUMBER**

NASA CR-191511
ICASE Report No. 93-51

**11. SUPPLEMENTARY NOTES**

Submitted to Phys. Review E

Langley Technical Monitor: Michael F. Card
Final Report

**12a. DISTRIBUTION/AVAILABILITY STATEMENT**

Unclassified - Unlimited

Subject Category 34

**12b. DISTRIBUTION CODE**

**13. ABSTRACT (Maximum 200 words)**

Reynolds stress closure models based on the recursion renormalization group theory are developed for the prediction of turbulent separated flows. The proposed model uses a finite wavenumber truncation scheme to account for the spectral distribution of energy. In particular, the model incorporates effects of both local and nonlocal interactions. The nonlocal interactions are shown to yield a contribution identical to that from the $\epsilon$-RNG, while the local interactions introduce higher order dispersive effects. A formal analysis of the model is presented and its ability to accurately predict separated flows is analyzed from a combined theoretical and computational stand point. Turbulent flow past a backward facing step is chosen as a test case and the results obtained based on detailed computations demonstrate that the proposed recursion -RNG model with finite cut-off wavenumber can yield very good predictions for the backstep problem.

**14. SUBJECT TERMS**

Reynolds stress model; Renormalization group; turbulent separated flows

**15. NUMBER OF PAGES**

31

**16. PRICE CODE**

A03

| 17. SECURITY CLASSIFICATION OF REPORT<br>Unclassified | 18. SECURITY CLASSIFICATION OF THIS PAGE<br>Unclassified | 19. SECURITY CLASSIFICATION OF ABSTRACT | 20. LIMITATION OF ABSTRACT |
|---|---|---|---|